

# Target Multipaths in WiFi-based Passive Radars



By

**Haroon Mazhar**

**NUST201260858MSEEC61212F**

Supervisor

**Dr. Syed Ali Hassan**

**Department of Electrical Engineering**

A thesis submitted in partial fulfillment of the requirements for the degree  
of MSEE

In

School of Electrical Engineering and Computer Science,  
National University of Sciences and Technology (NUST),

Islamabad, Pakistan.

(December 2014)

# Approval

It is certified that the contents and form of the thesis entitled “**Target Multipaths in WiFi-based Passive Radars**” submitted by **Haroon Mazhar** have been found satisfactory for the requirement of the degree.

Advisor: **Dr. Syed Ali Hassan**

Signature: \_\_\_\_\_

Date: \_\_\_\_\_

Committee Member 1: **Dr. Adnan Khalid**

Signature: \_\_\_\_\_

Date: \_\_\_\_\_

Committee Member 2: **Dr. Muhammad Shahzad**

Signature: \_\_\_\_\_

Date: \_\_\_\_\_

Committee Member 3: **Dr. Amir Ali Khan**

Signature: \_\_\_\_\_

Date: \_\_\_\_\_

# Abstract

In recent years there has been a growing interest in passive radars due to abundant availability of variety of communication signals which are used to detect the targets. This research is focused towards urban sensing applications of passive radars using WiFi signals. The effects on the range measurement accuracy of a WiFi-based passive radar has been investigated in scattering rich urban environment. In WiFi based passive radars, when multiple copies of signal from the same target are received due to propagation through a rich scattering environment, various range measurement inaccuracies are induced including offset of the target from its true range, smearing of the target in range dimension or appearance of ghost targets. Relationship between range measurement inaccuracies due to target multipaths and range resolution of transmission waveform has been studied. WiFi waveforms have been generated using computer simulation and fully functional passive radar processing scheme has been developed to study the effects of multipaths in different setups. To combat the effects of target multipaths equalization process has been successfully applied in the target channel thus to determine the true ranges of targets. An algorithm has been proposed which is based on two step solution, i.e., signal separation followed by equalization, to mitigate the effects of multipaths in WiFi-based passive radars.

# Certificate of Originality

I hereby declare that this submission is my own work and to the best of my knowledge it contains no materials previously published or written by another person, nor material which to a substantial extent has been accepted for the award of any degree or diploma at NUST SEECS or at any other educational institute, except where due acknowledgement has been made in the thesis. Any contribution made to the research by others, with whom I have worked at NUST SEECS or elsewhere, is explicitly acknowledged in the thesis.

I also declare that the intellectual content of this thesis is the product of my own work, except for the assistance from others in the project's design and conception or in style, presentation and linguistics which has been acknowledged.

Author Name: **Haroon Mazhar**

Signature: \_\_\_\_\_

# Acknowledgment

I would like to express my most sincere gratitude to my thesis supervisor, Dr. Syed Ali Hassan, for his continuous guidance and support during my research work. I truly appreciated all the time and advice he gave me, which helped me overcome many difficulties along the way in order to complete this thesis.

I would like to show my thankfulness to my wife, without whose support I would have never reached this point. I am also thankful to my children, Ahmed and Hadia, for giving me the time to pursue a project like this one. Most importantly I am grateful to my wonderful parents for their unending prayers, support and encouragements throughout my life.

Above all, I am grateful to Allah Almighty for granting me the strength and abilities to successfully complete this study.

# Table of Contents

<b>1</b>	<b>Introduction</b>	<b>1</b>
1.1	History of Passive Radars . . . . .	3
1.2	Problem Statement . . . . .	4
1.3	Organization of Thesis . . . . .	5
<b>2</b>	<b>Passive Radar Theory</b>	<b>6</b>
2.1	Bi-static Geometry . . . . .	6
2.2	Radar Equation . . . . .	7
2.3	Target Localization . . . . .	8
2.4	Radar Performance . . . . .	9
2.4.1	Range Resolution . . . . .	9
2.4.2	Range Ambiguity . . . . .	9
2.4.3	Doppler Resolution . . . . .	10
2.4.4	Doppler Ambiguity . . . . .	10
<b>3</b>	<b>Literature Review</b>	<b>11</b>
<b>4</b>	<b>Signal and Channel Model</b>	<b>15</b>
4.1	Signal Model . . . . .	15
4.2	Channel Model . . . . .	17

<i>TABLE OF CONTENTS</i>	vi
<b>5 Ambiguity Function</b>	<b>19</b>
5.1 Ambiguity Function of GSM Signal . . . . .	20
5.2 Ambiguity Function of WiFi Signal . . . . .	23
<b>6 Passive Radar Processing</b>	<b>24</b>
6.1 Reference Channel . . . . .	24
6.1.1 Equalization . . . . .	25
6.2 Target Channel . . . . .	25
6.2.1 Subtraction . . . . .	27
6.2.2 Cross Correlation . . . . .	27
6.2.3 Detection . . . . .	27
6.3 Assumptions . . . . .	27
<b>7 Simulation Setup and Results</b>	<b>29</b>
7.1 Setup 1: Single Target-Single Scatter . . . . .	29
7.1.1 Results . . . . .	31
7.2 Setup 2: Single Target-Multiple Scatters . . . . .	32
7.2.1 Results . . . . .	32
7.3 Setup 3: Multiple Targets-Multiple Scatters . . . . .	33
7.3.1 Results . . . . .	33
<b>8 Equalization for Target Multipath</b>	<b>34</b>
8.1 Equalization Problem . . . . .	34
8.2 Equalization Steps . . . . .	35
8.3 Proposed Algorithm . . . . .	36
8.4 Application . . . . .	37
<b>9 Conclusion</b>	<b>39</b>
9.1 Conclusion . . . . .	39

<i>TABLE OF CONTENTS</i>	vii
9.2 Major Contributions . . . . .	40
9.3 Future Work . . . . .	40
<b>A Matlab Code for Signal Generation</b>	<b>46</b>
<b>B 3D Ambiguity Function</b>	<b>55</b>
<b>C 1D Ambiguity Function</b>	<b>57</b>
<b>D Passive radar processing</b>	<b>59</b>

# List of Figures

1.1	Passive radar products . . . . .	4
2.1	Bistatic Target Geometry . . . . .	6
2.2	Constant range counter . . . . .	7
2.3	Localization with DOA . . . . .	8
2.4	Localization with Multistatic Configuration . . . . .	9
4.1	Simulated WiFi Beacon Signal . . . . .	16
5.1	Simulated GSM frame . . . . .	20
5.2	Ambiguity function of GSM Signal . . . . .	21
5.3	Ambiguity function of WiFi Signal . . . . .	22
6.1	Passive Radar Processing . . . . .	25
7.1	Target environment model for setup 1 . . . . .	29
7.2	Range measurement inaccuracies as a result of multipath . . . . .	30
7.3	2D Cross ambiguity function of setup 3 . . . . .	33
8.1	Process diagram for target detection in two phases . . . . .	36
8.2	Offset target equalized for setup 1 . . . . .	37
8.3	Smearred target equalized for setup 2 . . . . .	38

# List of Tables

7.1	ITU Office Channel Model . . . . .	32
-----	------------------------------------	----

# Chapter 1

## Introduction

Passive radars, also known as Passive Coherent Location (PCL) systems, operate on the principle of bi-static radar and instead of transmitting their own signals, utilize the transmissions of other non-cooperative sources, like telecommunication signals, to detect the targets. In bi-static radar the transmitter and receivers are located at geographically disperse locations. Due to abundance of communication signals in the environment, there is a growing interest in passive radars which offer many fold advantages over conventional radars. The signal sources for passive radars are also known as “illuminators of opportunity” which are are exploited to measure the range and velocity of targets. The availability of these constant sources of illuminations makes passive radars an attractive option due to low cost of designing, manufacturing and operating the system. The advantages offered by passive radars are listed below:-

- The system requires minimal operating power as there is no high power transmissions.
- No frequency bandwidth allocation is required for passive radars which

means that this freed up expensive frequency band can be used for commercial applications.

- Mostly phased array antennas are used in receiving the target echoes so there are no mechanically moving parts thus it has higher reliability than conventional radars.
- Passive radar does not transmit any signal hence it is covert to enemies signal intelligence system thus immune to jamming and Anti-Radiation Missile (ARM) attacks.
- Passive radars mostly operate on low frequency bands thus they have inherent capability to detect the stealth targets because stealth measures are designed for specific radar frequency bands.
- Using signal processing techniques, advance features of the targets like track generation, target identification and synthetic aperture imaging can also be extracted using passive radars.

The drawback of passive radars is that, geometry of is more complicated as compared to conventional radars, due to different locations of transmitter and receiver. Also, the transmitted waveform is not in direct control of passive radar designer and most of the communication signals are not well suited for target detection, hence a given waveform may be suitable for only a particular application and extra signal processing is required to extract target environment information.

Applications of passive radars may include:

- Low Cost Air Traffic Control (ATC) Systems
- Law Enforcement (Traffic Monitoring)

- Border Crossing/Intrusion Detection
- Through the Wall (TTW) target detection
- Detection of Stealth Targets
- Local Metrological Monitoring
- Planetary Mapping

## 1.1 History of Passive Radars

The first practical passive radar was deployed by Germans in 1943 known as Klein Heidelberg [12] which comprised of receivers installed along the channel coast line to exploit the emission of British Chain Home radars. Much of the interest in the passive radars was lost after the invention of mono-static active radars which offered greater advantage over bi-static counterparts [20]. The research interest revived in passive radars revived in 1990s when sufficient computing power was available to carry out complex signal processing of passive radars and many advantages offered by this low cost technology. First commercial system Silent Sentry was introduced by Lockheed-Martin, USA which detect aerial targets by using illuminations of commercial FM radio broadcast. Currently, number of products are available in market operating on passive radar principal and utilizing various illuminations of opportunity like, AULOS from Selex ES Italy, Silent Guard from ERA Czech Republic, Homeland Alerter 100 from Thales France, CELLDAR based on GSM Signals from Roke Manor Research, UK etc.

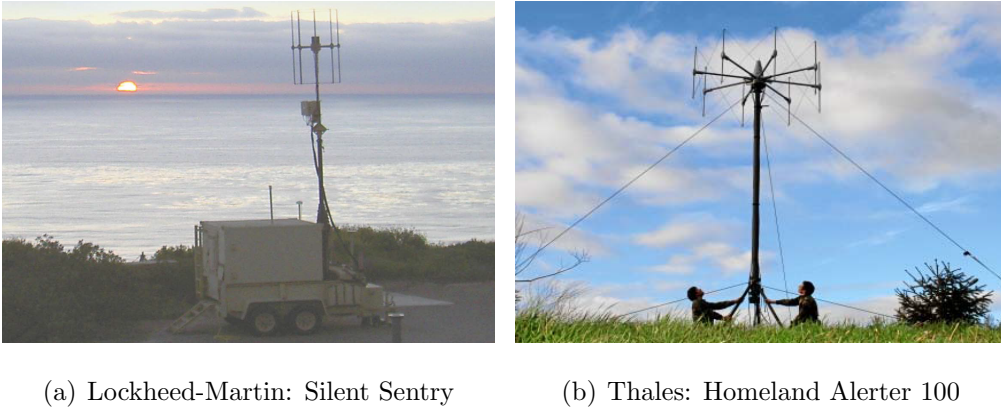


Figure 1.1: Passive radar products

## 1.2 Problem Statement

Long range surveillance applications of passive radars, using various analog and digital waveforms, have reached to a point of maturity and practical systems have started to appear in market for various defense and civil applications. Because of many advantages offered by the passive radars, there is a growing interest to utilize them in urban and indoor sensing environment for detection of human or vehicular targets.

Active research is going on to utilize the WiFi waveforms for passive radars in urban applications. In a WiFi-based urban sensing passive radar, the multipaths cannot be ignored and will cause range measurement errors. Primary reason is the geometry of the environment, in which all signals are received in two dimensional plane where, despite of significant path length difference in-between direct and multipath signals, considerable power is received in multipath signal returns. In contrast, for aerial target detection application, signals are received in three dimensions due to height of aircraft and possible scatter objects are located near the receiver, which cause negligible path length difference in-between direct and reflected paths.

This thesis is focused towards thoroughly investigating the target multipaths problem in a WiFi-based passive radar and the type of range measurement errors they may introduce. An equalizer solution is also proposed and implemented to combat the multipath errors thus to determine the true range of the target in rich scattering environment.

### 1.3 Organization of Thesis

Chapter 2 gives an overview of passive radar theory including the range equation, geometry consideration and target localization. The research work going on in area of passive radar is reviewed in Chapter 3.

Ambiguity function is used to analyze the suitability of waveform of any illumination of opportunity for PCL applications and is also used to determine the target parameters. The implementation details of ambiguity function is given in Chapter 5.

The signal and channel model developed is presented in Chapter 4 while the passive radar processing scheme implemented to study the effects of multipaths is given in Chapter 6. The target environment simulation with results are presented in Chapter 7.

Lastly, solution to multipath problem is proposed and implemented in Chapter 8. The Matlab codes are attached as appendix to the report.

# Chapter 2

## Passive Radar Theory

### 2.1 Bi-static Geometry

Passive radars are a type of bi-static radars hence all the underlying theory is same for both. In bi-static radar the transmitter and receiver are located at different locations as illustrated in figure 2.1. The transmitter  $T_x$  and receiver

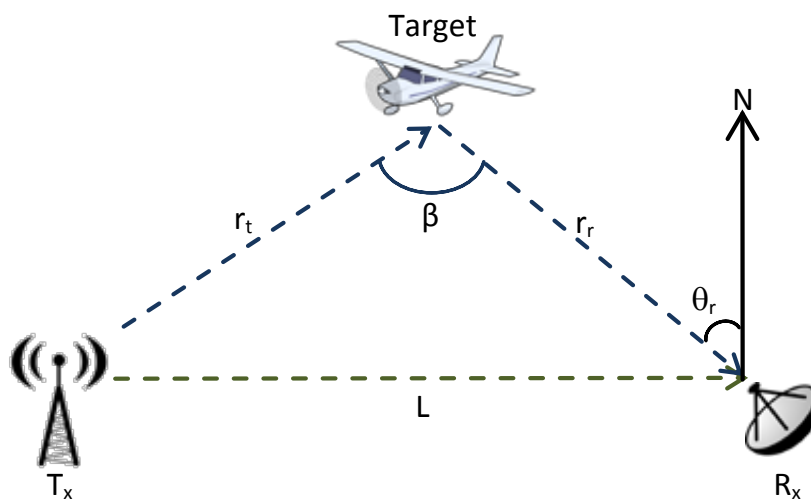


Figure 2.1: Bistatic Target Geometry

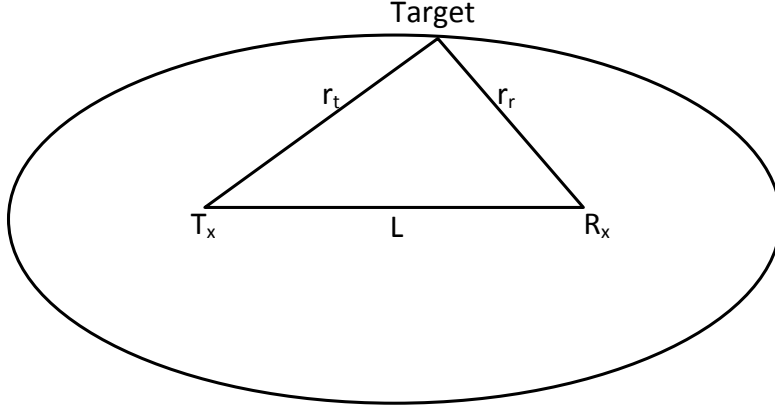


Figure 2.2: Constant range counter

$R_x$  are separated in distance through baseline  $L$ . The sum of transmitter-target distance  $r_t$  and receiver-target distance  $r_r$  is known as bi-static range  $R_{bistatic} = r_t + r_r$ . Angle  $\theta_r$  is with reference to geographical north.

The target range is given by

$$r_r = \frac{(r_t + r_r)^2 - L^2}{2(r_t + r_r + L \sin \theta_r)} \quad (2.1)$$

The range  $r_r$  cannot be directly calculated as angles involved in the geometry are unknown [31]. A passive radar normally calculates the  $R_{bistatic}$  which is proportional to total signal propagation time from transmitter to receiver. It is noted that measured bistatic range forms an ellipse with the transmitter and receiver as the two foci as illustrated in Figure 2.2.

$$r_t + r_r = \text{constant} \quad (2.2)$$

## 2.2 Radar Equation

The power received at a passive radar receiver [13] is given by

$$P_r = \frac{P_t G_t G_r \lambda^2 \sigma_B}{(4\pi)^3 r_t^2 r_r^2} \quad (2.3)$$

where  $P_r$  is the received signal power,  $P_t$  is the transmit power,  $G_t$  is the transmit antenna gain,  $G_r$  is the receive antenna gain,  $\sigma_B$  is the target bistatic radar cross section (RCS) area, and  $\lambda$  is the radar wavelength.

## 2.3 Target Localization

The target localization in bi-static radar can be done either by getting the direction of arrival (DOA) of signal using directional antenna which enable determining the angle involved in equation 2.1 and thus localizing the target in x-y plane. The DOA method is depicted in Figure 2.3. Alternatively a multistatic configuration can be deployed with each  $T_x$  and  $R_x$  pair providing a constant bi-static range ellipse. The ellipses from each pair will intersect with each other at target location as shown in Figure 2.4.

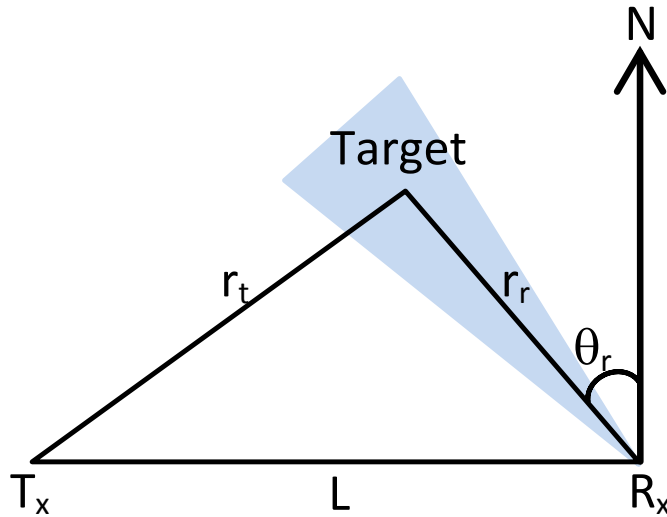


Figure 2.3: Localization with DOA

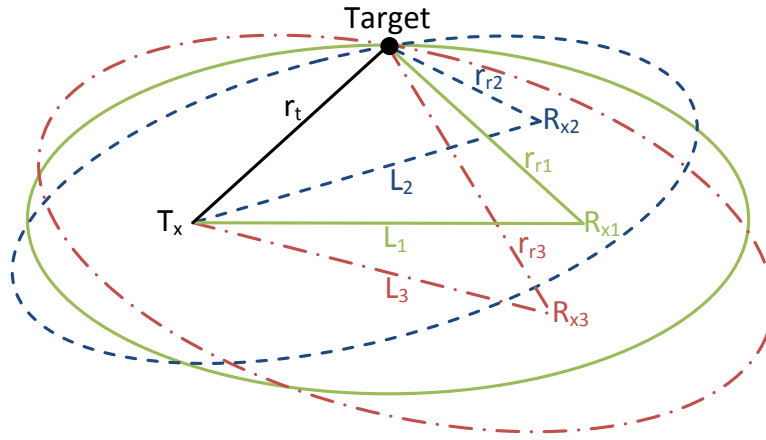


Figure 2.4: Localization with Multistatic Configuration

## 2.4 Radar Performance

### 2.4.1 Range Resolution

Range resolution of the radar is the ability to distinguish two or more closely located targets. It is a function of signal bandwidth. More the signal bandwidth greater the capability of radar to distinguish two targets. Denoting speed of light in m/s by  $c$  and bandwidth of the signal in Hz by  $B$  the range resolution is given by  $R_{res} \approx c/B[m]$ .

### 2.4.2 Range Ambiguity

Due to repetitive structure of waveforms e.g. pulse in active radars which are transmitted at fix pulse repetition frequency (PRF) or periodic synchronization signals in communication waveforms, ambiguity in ranges may arise. This will result in energy received in the return signal at a time instance which does not correspond to actual target and may be detected as a target.

### 2.4.3 Doppler Resolution

Doppler frequency is associated with the speed of target. The ability of radar to distinguish between two different Doppler frequency tones in received signal is known as Doppler resolution. In other words, it is ability of radar to distinguish between two targets, moving at different speeds. Doppler resolution is inversely related to the observation time. The greater the observation time  $t$ , the finer the frequency resolution.  $\Delta f_D \approx 1/t[\text{Hz}]$ .

### 2.4.4 Doppler Ambiguity

Similar to range ambiguity, Doppler ambiguity can also arise due to modulation of some kind on the transmitted signal. These ambiguities appear along Doppler dimension and may lead to detection of ghost targets.

# Chapter 3

## Literature Review

Ambiguity function is used to analyze the suitability of waveform of any illuminator of opportunity for PCL applications. The achievable range and Doppler resolution achievable are calculated as a function of delay and velocity. Baker et al. [1] compared the performance of commercial FM analogue radio, GSM and Digital Audio Broadcast (DAB) signals in terms of sensitivity and achievable target detection range. The authors reported that FM transmissions are ideal for long range aerial target detection flying at medium altitude due to higher transmissions power of FM broadcast stations. The GSM signals are ideal for tracking vehicles and monitoring movements around building because GSM antennas are mostly installed in look down manner with limited radiate power. The DAB stations transmit power level comparable to FM broadcast however range is less due to more attenuation at higher operational frequency. Some authors analyze the waveforms of analogue FM broadcast, GSM signals and analogue TV broadcast using ambiguity function to determine the range and Doppler resolutions of this candidate illuminator of opportunity. They have reported that FM broadcast has highly variable range resolution depending upon signal bandwidth which

changes with broadcasted program contents. GSM and TV signals have very detailed structures however range resolution is poor if complete signal is used for PCL applications due to repetitive contents at fixed period.

Various digital waveforms have been analyzed by the researchers for feasibility of utilizing them as illuminators of opportunity for passive radars. Coleman et al. [5] analyzed Digital Audio Broadcast (DAB) and Digital Radio Mondiale (DRM) as candidate waveforms for PCL applications. They have reported that DAB is suitable for detection of aircraft due to detailed waveform structure and constant bandwidth. DRM can also be used for same purpose but the range resolution is poor due to narrow bandwidth in comparison to DAB. Palmer et al. [21] have carried out the ambiguity function analysis of Satellite Digital Video Broadcast (DVB-S) and Terrestrial Digital Video Broadcast (DVB-T) and developed an algorithm known as modified CLEAN to iteratively cancel signals in time domain before the formation of Doppler and range map for ambiguity function analysis. Tan et al. [30] have analyzed GSM signal in details for passive radar application and further demonstrated a system capable of detecting movements of vehicles. Berger et al. [2] have analyzed the OFDM wave forms and have formulated matched filter equation for OFDM waveforms equivalent to Fourier analysis based on assumption that phase rotation due to Doppler is content in time domain.

Homer et al. [14] proposed a SAR based on Low Earth Orbit (LEO) satellites. Samczynski et al. [22] has proposed passive radar based on GSM signal for traffic monitoring and extraction of traffic features like road capacity, average speed of cars etc. They have argued that GSM signals can be used for low altitude and ground targets only as the signal from GSM base stations have small emissions in upper hemisphere due to sector anten-

nas which have beams pointed towards ground. Sun et al. [29] have shown passive radars based on GSM signals have application in various scenarios e.g. traffic monitoring, air and coastal surveillance, and motion detection through-the-wall. They have developed multistatic radar network for large area air surveillance however they have highlighted that due to inherent limitations of GSM waveforms it is not practical to replace traditional active radars with GSM passive radars. Furthermore in [28] same researchers have shown that that detection range of passive radar is much larger than the service area of given base station. They have also estimated the target Radar Cross Section (RCS) area of airborne target against GSM passive radar in same paper.

Clone et al. [10] have thoroughly analyzed the ambiguity functions of various WiFi standards to determine their suitability for passive radar applications. The research indicate that the range resolution performance is dominated by periodic beacon signals and theoretical range resolution ( $R_{res}$ ) is of the order of 25m, whereas the velocity resolution of 0.2 m/s can be achieved using target integration time of 0.6s, which is reasonable to detect slow moving human targets. Chetty et al. [4] have demonstrated low cost through the wall (TTW) passive radar system using WiFi signals to detect human targets from stand off distances. Clone et al. have experimented with WiFi waveforms to detect human and vehicular targets in indoor and outdoor environments [6], moreover, they applied the inverse synthetic aperture radar (ISAR) technique for detection and tracking of vehicles through high-resolution cross-range profiling [9]. They also addressed the 2D localization in a WiFi-based passive radar using multiple receivers in [11].

In a rich scattering urban environment, the reflected signal from the target can reach the passive radar receiver through multiple paths, because of

reflections from surrounding scatter objects. These multiple copies of the signal from the same target, combine vectorially at the receiver to give rise to constructive or destructive interference, which may seriously degrade the range measurement accuracy of passive radar. In active radars, the multipaths errors are sometimes called *low-angle tracking errors*, which arise due to signal bouncing off from smooth ocean or earth surface giving rise to ghost targets [26]. Sutlur et al. have extensively researched on multipath model, and its further exploitation, in TTW active radars [25][24]. Researchers have also faced range measurement errors in WiFi-based passive radars due to target multipaths [4][11], however, same was ignored in both the works. Although Chetty et al. [4] introduced the target multipaths in their initial mathematical model, however, it was neglected to simplify the discussion which resulted in erroneous range measurement in their TTW passive radar experiment.

# Chapter 4

## Signal and Channel Model

### 4.1 Signal Model

The omnipresence of different variants of IEEE 802.11-based wireless local area networking (WLAN) signals make them a suitable transmissions of opportunity for indoor and urban sensing applications of the passive radars. IEEE 802.11 a,b,g and n standards are most prolific waveforms found in urban environment to provide WLAN connectivity of up to 600 MHz, using mix of orthogonal frequency-division multiplexing (OFDM) and direct-sequence spread spectrum (DSSS) modulations in 2.5 and 5 GHz industrial, scientific and medical (ISM) radio frequency bands.

To study the effects on range measurement accuracy of passive radar, when multiple delayed copies of signal are received from a target in a rich scattering environment, 802.11 WLAN signal has been simulated and analyzed. IEEE 802.11a standard operates in 5 GHz whereas IEEE 802.11 b and g standards operate in 2.4 GHz ISM frequency bands, with a maximum data rate capacity of 11 Mbps for 802.11b standard and 54 Mbps for 802.11a/g standards, by utilizing a mix of DSSS and OFDM modulations and channel

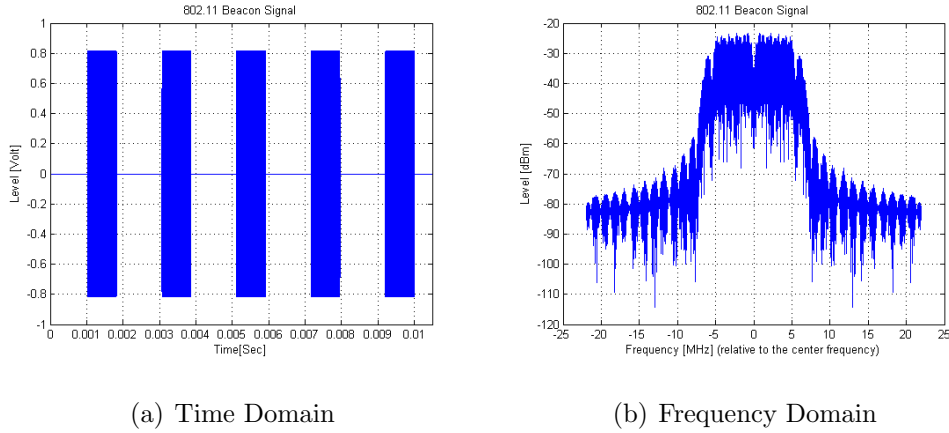


Figure 4.1: Simulated WiFi Beacon Signal

bandwidth of 20 MHz [15]. Recently 802.11n standard has become popular which can support maximum data rate of 600 Mbps by utilizing multiple-input and multiple-output (MIMO) antennas in 2.4 /5 GHz frequency bands, channel bandwidth of 40 MHz and OFDM modulation.

The 802.11 a/b/g WiFi signals are dominated by the beacon signals, which uses DSSS modulation and this study is based on using beacon frames for passive radar application. Beacon frame is a type of management frame which is periodically transmitted to announce the presence and capabilities of wireless access point (AP). Beacon frames are transmitted at regular intervals using lowest data rate of operating standard of AP. Each simulated beacon frame contains Physical Layer Convergence Protocol (PLCP) preamble (128 bit long preamble and 16 bit start frame delimiter), 48 bit PLCP header and payload data. The baseband data is modulated at 1 Mbps using differential binary phase shift keying (DBPSK) and length 11 barker code [+1, 1, +1, +1, 1, +1, +1, +1, 1, 1, 1] is later applied to spread the signal [15]. The simulated beacon frames are transmitted on frequency channel 6 (2437 MHz) at an interval of 1024 microseconds. The data set used for passive radar simulation is 10 ms long which contains 5 beacon frames each of 0.79 ms and

sampling frequency ( $F_s$ ) is set to 88 MHz (sample time  $T_s = 1/F_s$ ). The simulated signal is shown in Figure 4.1.

## 4.2 Channel Model

A propagation channel model is created to simulate the location of targets and multipath scattering objects using

$$h(t) = \sum_{n=1}^N C_n e^{j(\phi_n - 2\pi c\tau_n/\lambda_c + 2\pi f_{D_n}t)} \delta(t - \tau_n) \quad (4.1)$$

where  $h(t)$  is channel response,  $C_n$  is complex gain which depends upon cross section area of target or scattering object,  $\phi_n$  is random phase induced on the signal by the reflecting object and assumed to be uniformly distributed between  $[-\pi, \pi]$ ,  $c$  is speed of light,  $\tau_n$  is the delay due to location of target or multipath scatter,  $\lambda_c$  is the wavelength of transmitted signal and  $f_{D_n}$  is the Doppler frequency induced due to velocity of target [27].  $N$  is total number of reflecting objects, including both targets and scattering objects, available in the environment. It is assumed that only static scattering objects are available, hence all returns, including direct and multipath, from a single target will have same Doppler frequency  $f_{D_n}$  but will vary in  $\tau_n$  depending upon location of target and multipath scattering objects.  $\tau_n$  corresponds to bistatic ranges  $R = c\tau_n$  implying that it is sum of distances between transmitter to target and target to receiver, for direct target reflection and additional multipath length is added for multipath. The received signal in target channel of the receiver is convolution of transmitted waveform and channel response given by following equation.

$$s(t) = u(t) * h(t) \quad (4.2)$$

where  $s(t)$  is the signal received in target channel of passive radar,  $u(t)$  is the transmitted waveform and  $*$  denotes the convolution operation.

# Chapter 5

## Ambiguity Function

The self ambiguity function, which is a correlation function of same signal with time delayed and Doppler shifted copies, is used to analyze the suitability of any waveform for radar applications. The ambiguity function of simulated signal is calculated using

$$\chi(\tau, f_D) = \left| \int_{-\infty}^{\infty} u(t)u^*(t - \tau)e^{-2\pi j t f_D} dt \right|^2 \quad (5.1)$$

where  $\tau$  is time delay and  $f_D$  is the Doppler frequency. The given equation can be implemented by three approaches [18].

1. Fast Fourier Transform (FFT) method
2. Cross correlation method
3. Double summation method

The first two approaches require lesser computational power as compared to third one, however the main disadvantages of these two are that the ambiguity function will be calculated for all possible  $f_D$  using FFT method and all possible  $\tau$  by using cross correlation method. In practical applications evaluation of only subset of  $\tau$  and  $f_D$  is required depending upon expected target

location, velocity and transmission characteristics. Hence in this study double summation method is implemented to evaluate the ambiguity function.

It is pertinent to highlight that due to large number of data points in simulated signals, it was beyond the capabilities of normal desktop computer to calculate the ambiguity function; hence 64 cores Solaris Cluster running Matlab 2009 was utilized which is available at High Performance Computing (HPC) lab of SEECS, NUST [23].

## 5.1 Ambiguity Function of GSM Signal

GSM normal burst down link signal was also simulated during course of research and the ambiguity function was analyzed to ascertain the correctness of implementation. The symbol period for GSM is 3.692s and 4 samples per modulator symbol out have been chosen. The user frame data assumed to be output of inter-leaver of 114 bit has been generated in each simulation cycle through random number generator; however in Time slot 1, the data is generated before the simulation cycles and same is used in all GSM burst. The normal burst has been constructed as per frame layout as per GSM

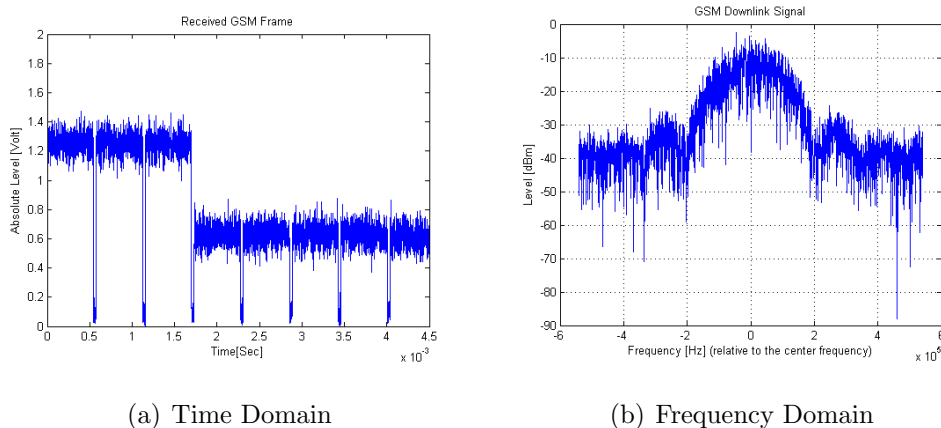
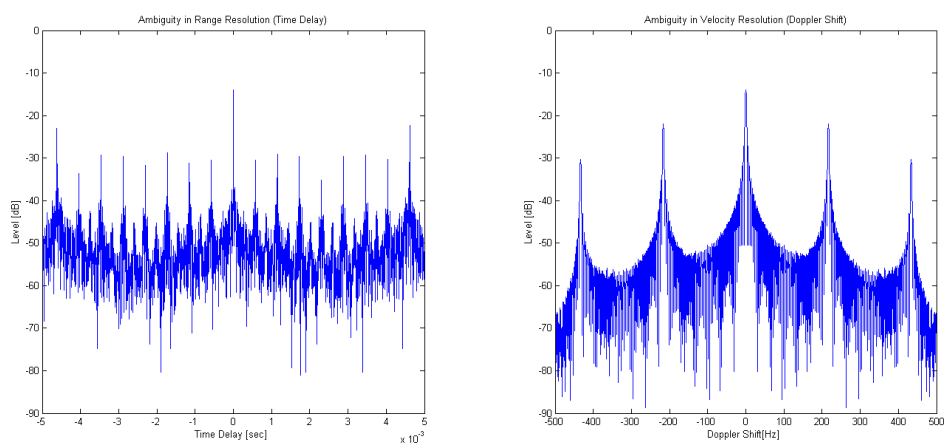
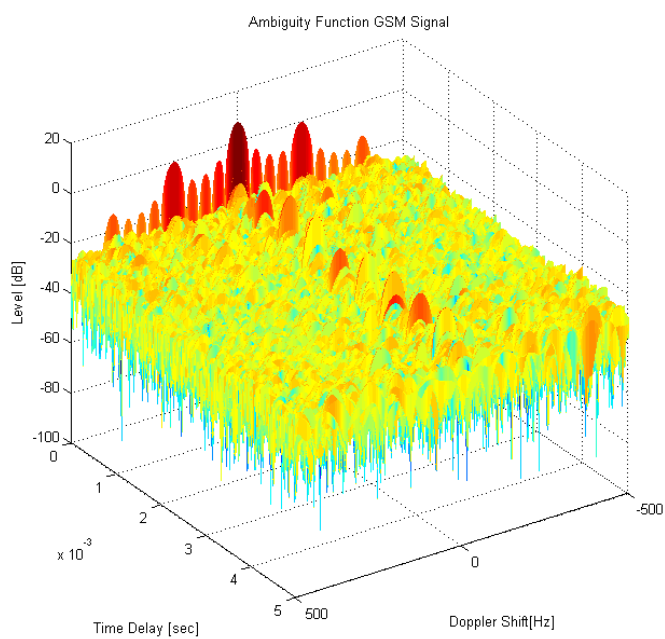


Figure 5.1: Simulated GSM frame



(a) Range Cut

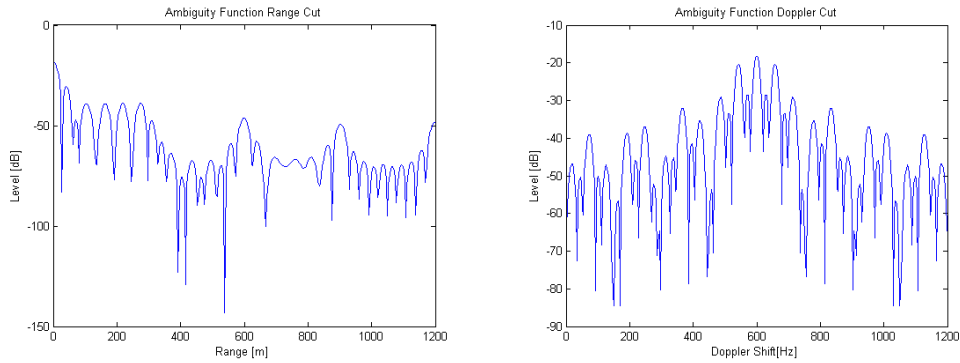
(b) Doppler Cut



(c) 3D Ambiguity Function

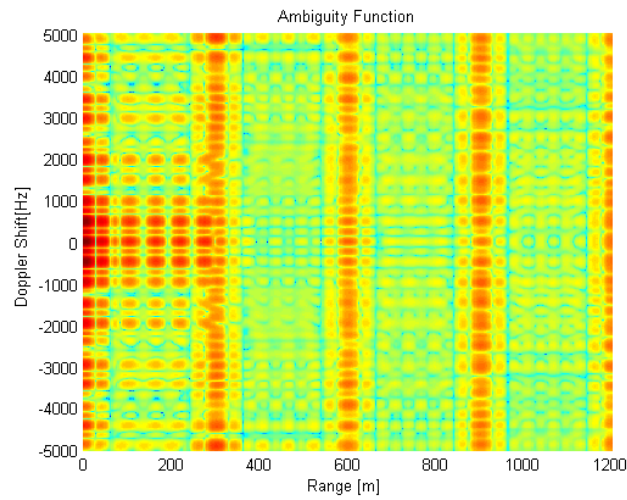
Figure 5.2: Ambiguity function of GSM Signal

specification. The simulation data has been generated for 0.25 seconds. The downlink power control algorithm has been applied so the amplitude of TS0, TS1 and TS2 is double then remaining slots. After each time slot silence



(a) Range Cut

(b) Doppler Cut



(c) 3D Ambiguity Function

Figure 5.3: Ambiguity function of WiFi Signal

period of 8.25 bit period has been inserted. Lastly simulated bits were modulated using GMSK modulation and channel impairments were added. The time domain view and spectrum simulated GSM frame is shown in Figure 5.1.

Ambiguity function of simulated GSM signal is shown in Figure 5.2. It is observed that the repetitive modulating signal contained in burst type GSM transmission is responsible for the range and Doppler ambiguities. After

every time slot there is ambiguity at 577 ms and its multiples moreover there is also ambiguity at 4.6 ms which is total frame time. In Doppler domain ambiguity is observed at 217 Hz Doppler velocities.

## 5.2 Ambiguity Function of WiFi Signal

The ambiguity function of 802.11 WiFi signals has been thoroughly analyzed in [10]. The ambiguity function of simulated WiFi beacon signals is shown in Fig. 5.3. The results are consistent with the study done in [10] which was carried out on actual WiFi 802.11b beacon signals.

# Chapter 6

## Passive Radar Processing

In this chapter, passive radar processing scheme is introduced, which has been followed to determine the effects of multipath target returns on range measurement accuracy of WiFi-based passive radar in urban environment. Generally two receiving channels are employed in a passive radar system as shown in Figure 6.1, one to receive the reference signal and the other one to receive the target returns.

### 6.1 Reference Channel

The signals received in reference channel can be defined by following equation

$$r(t) = A_{ref}u(t - \tau_{ref}) + \hat{n}(t) \quad (6.1)$$

where  $r(t)$  is the signal received in reference channel,  $u(t)$  is the transmitted waveform,  $A_{ref}$  is amplitude scaling factor and  $\tau_{ref}$  corresponds to wave propagation delay, which depends upon the distance between transmitter and receiver and  $\hat{n}(t)$  is the additive noise in receiving channel.

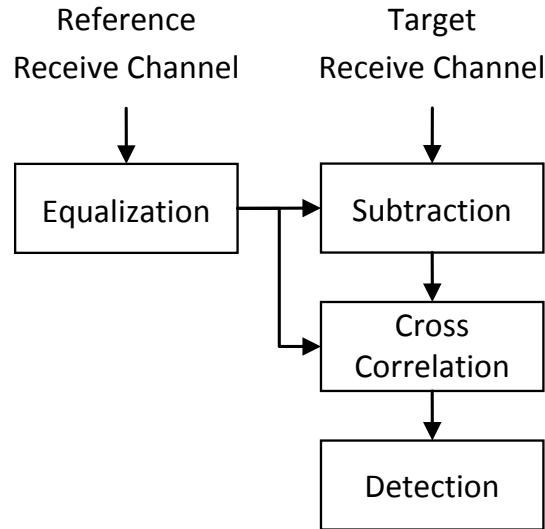


Figure 6.1: Passive Radar Processing

### 6.1.1 Equalization

In bistatic passive radars, the transmitter is not co-located with the receiver; thus the transmitted signal after passing through wireless channel experiences degradations, hence signal processing is required to be carried out to bring out the exact replica of transmitted waveform, which is to be utilized as reference signal.

## 6.2 Target Channel

The received signal in the target channel is the vector combination of direct signal and the multipath signals, hence the target signal will experience distortion, which will depend upon number of factors including

1. Location of scattering objects or extra path length multipath signals

have to travel.

2. Signal attenuation experienced by multipath signals after reflection.
3. The random phase  $\phi$  induced by scattering objects
4. The Doppler frequency of the target.

The signal received in target channel is given as

$$s(t) = \sum_{l=1}^L A_l u(t - \tau_l) e^{j2\pi f_{D_l} t} + \sum_{l=1}^L \sum_{m=1}^M A_{l_m} u(t - \tau_{l_m}) e^{j2\pi f_{D_l} t} + \sum_{c=1}^C A_c u(t - \tau_c) + A_{DSI} u(t - \tau_{DSI}) + \hat{n}(t) \quad (6.2)$$

where  $A$ ,  $\tau$  and  $f_D$ , with their given subscripts are corresponding amplitude scaling factors, time delays and Doppler frequencies, respectively. Following are the signal components received in target channel receiver

1. The first term corresponds to  $L$  targets to be detected by passive radar each having bistatic range equivalent to  $c\tau_l$  and target velocity which induces Doppler frequency  $f_{D_l}$ .
2. The second term corresponds to  $M$  multipaths encountered by signal after reflecting from  $L$  targets before reaching the passive radar target channel. In other words, the signal from each target is received through  $M$  multipaths.
3. The next term correspond to the reflections from  $C$  stationary clutters.
4. Direct signal interference (DSI), is the transmitted signal directly received in target channel.
5.  $\hat{n}(t)$  is the additive noise in the target receiving channel.

### 6.2.1 Subtraction

The reflections from static clutter and DSI are the major sources of performance degradation in passive radars and active research has been done in this area to counter their effects. A comparison of various clutter cancellation techniques is given in [3]. These signal components appear at 0 Doppler after cross correlation.

### 6.2.2 Cross Correlation

The target bistatic range and Doppler velocity is determined using cross-correlation function between  $s(t)$  and  $r(t)$  as follows

$$\chi[\tau, f_D] = \left| \sum_{n=0}^{N-1} s[n]r^*[n-i]e^{-2\pi jnf_D/F_s} \right|^2 \quad (6.3)$$

where  $N$  is the total number of samples collected which correspond to target integration time as  $NT_s$  and  $i$  is the time bin corresponding to time delay  $\tau = iT_s$ .

### 6.2.3 Detection

After 2D correlation targets are detected using some kind of detection algorithm e.g. continuous far alarm rate (CFAR).

## 6.3 Assumptions

In this study, it is assumed that i) perfect replica of transmitted waveform is available at reference channel thus  $r(t) = u(t)$ , ii) reflections from stationary clutter and DSI have been perfectly subtracted from signal received in target

channel [3], iii) sufficient signal-to-noise ratio (SNR) is available to nullify any effects of  $\hat{n}(t)$ .

# Chapter 7

## Simulation Setup and Results

To accurately determine the effects of multipaths on range measurement capability of urban WiFi-based passive radar, following simulation scenarios have been studied.

### 7.1 Setup 1: Single Target-Single Scatter

In the first setup, a single target is present in the environment having bistatic range of 68.18m and a Doppler frequency of 50 Hz, along with one scattering

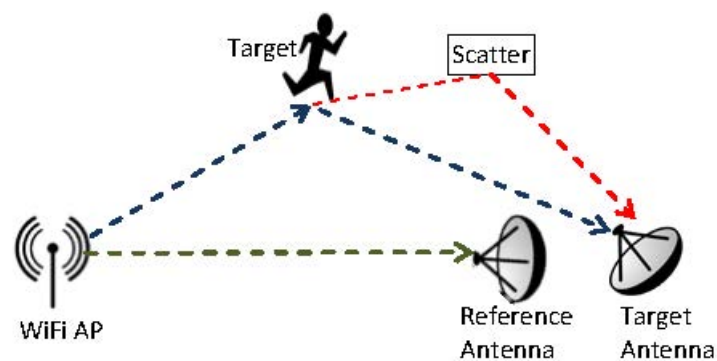


Figure 7.1: Target environment model for setup 1

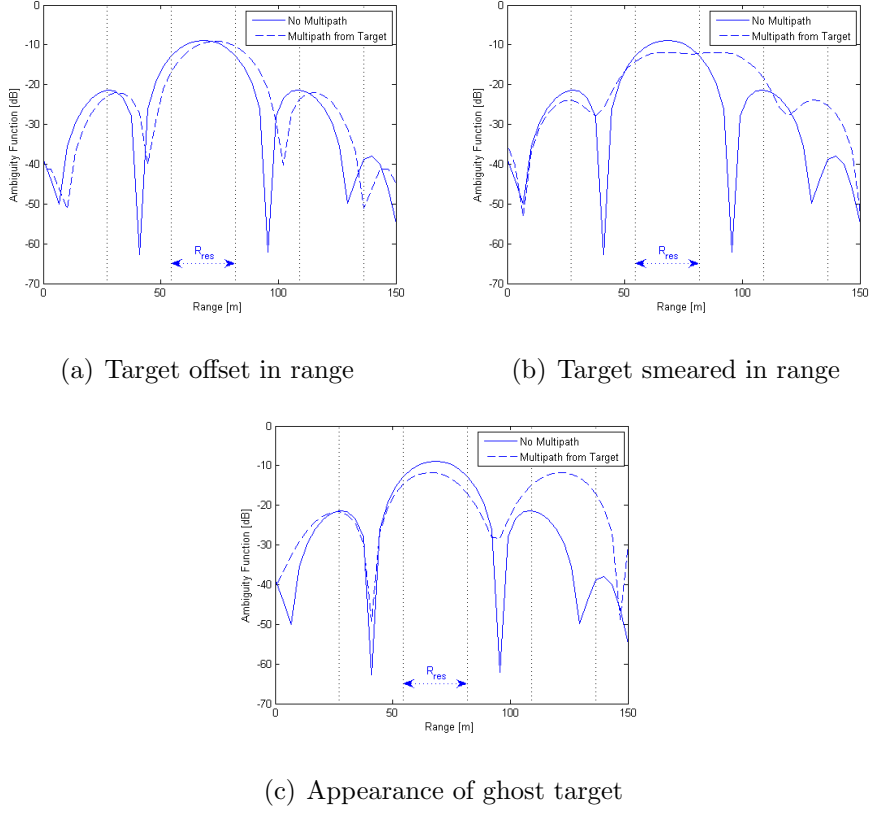


Figure 7.2: Range measurement inaccuracies as a result of multipath

object to give rise to a multipath. The target environment of this setup is depicted in Fig. 7.1. Based on this setup and using the assumptions mentioned in the previous section, the signal received in target channel can be written as

$$s(t) = Au(t - \tau)e^{j2\pi f_D t} + A_m u(t - \tau_m)e^{j2\pi f_D t}. \quad (7.1)$$

It is to be noted that the Doppler frequency in both the terms remains the same as the multipath reflection is from stationary scattering object. To observe the effects on range measurement accuracy of the simulated model, the scatter object was moved to various distances.

### 7.1.1 Results

The cross ambiguity function in (6.3) is shown in Fig. 7.2, at 50 Hz Doppler cut, for various positions of the scattering object. The solid plot depicts the range measured in the absence of any multipath whereas the dotted plot is the error induced when signal also travels through a multipath after reflection from the static scattering object. As a result of distorted target signal, the resultant target range peak will either be **offset** from the true range {Fig. 7.2(a)} or the target will **smear** in range dimension {Fig. 7.2(b)} or **ghost** targets will appear which may not necessarily correspond to actual direct and scatter path lengths {Fig. 7.2(c)}.

However, the resultant range plot, among depicted plots, will be temporal due to movement of target since small change in the location of target will result in large phase variation for both direct and multipath signal [27].

The appearance of offset, smeared or ghost target in range dimension of ambiguity plot is also dependent upon path length difference ( $\Delta R$ ) between direct and reflected signal path and has been analyzed in relation to radar range resolution ( $R_{res}$ ). Based on number of simulation runs it has been observed that,

- If  $\Delta R < R_{res}$  all three types of range distortion may appear Fig. 7.2(a)-7.2(c).
- If  $R_{res} < \Delta R < 2R_{res}$  all three types of range distortion may also appear Fig. 7.2(a)-7.2(c),
- In case of  $\Delta R > 2R_{res}$  ghost targets will only appear, as shown in Fig. 7.2(c).

Table 7.1: ITU Office Channel Model

Relative Delay (ns)	Average power (dB)
0	0
50	-3
110	-10
170	-18
290	-26
310	-32

## 7.2 Setup 2: Single Target-Multiple Scatters

In this setup, again a single target is simulated to be present in the environment, however the radio propagation channel used is a standard ITU Indoor Office Channel Model A [17]. The path delays and the average power of this channel are given in Table 7.1. The RMS delay spread of this channel model is  $35ns$  which correspond to  $\Delta R = 10.5m$  and is less than  $R_{res}$  of selected waveform.

### 7.2.1 Results

The simulation results of this setup is also consistent with the findings for Setup 1. As the RMS delay spread is less than the  $R_{res}$  of the signal, the distorted received signal in target channel of passive radar resulted in all three range measurement inaccuracies, i.e offset, smear and ghost, which are shown in Fig. 7.2.

## 7.3 Setup 3: Multiple Targets-Multiple Scatterers

In this scenario two targets are simulated in rich scattering environment. One target, having Doppler frequency of 70Hz, is situated at 770m with 2 multipaths at  $\Delta R_1 = 10$  and  $\Delta R_2 = 20m$ ; whereas other target is at 550m with a Doppler frequency of -50Hz, having only strong specular waveform and no multipath reflections. The 2D cross ambiguity function is shown in Fig. 7.3.

### 7.3.1 Results

It has been observed that, given high Doppler resolution is achieved using long target integration time, multipaths arising from one target do not influence the range measurement accuracy of other targets.

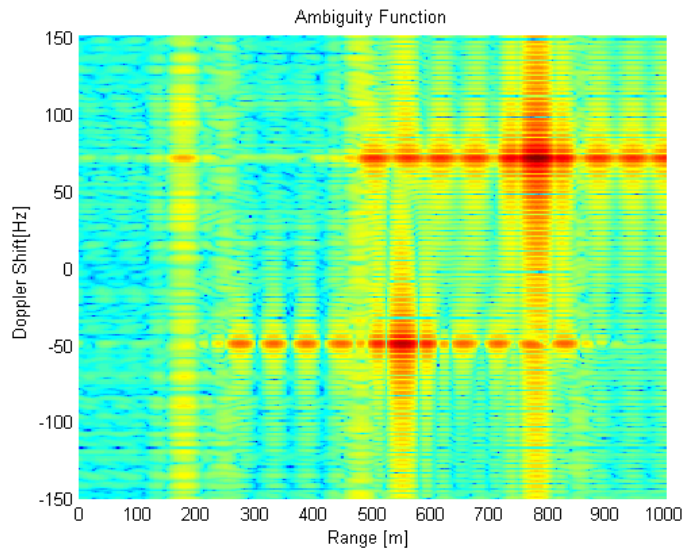


Figure 7.3: 2D Cross ambiguity function of setup 3

# Chapter 8

## Equalization for Target Multipath

Based on the results of previous section and experiments of other researchers [4], it has been established that the target multipaths seriously degrade the performance of WiFi-based passive radar in urban sensing environment.

### 8.1 Equalization Problem

Equalization of target multipaths is not a straight forward problem due to multiple challenges. The wireless propagation channel can not be known in advance, as all the targets in the environment are, in fact, the moving scatter objects, moreover, this channel is time varying due to the movement of targets. Signal received in the target channel of passive radar is a linear combination of all targets returns and associated multipaths (6.2). In other words,  $h(t)$  in (4.1) is the aggregate channel response of all targets. As each target along with its associated multipaths presents a different channel to the receiver, signal returns associated with target of interest are required to be

extracted from  $s(t)$  and then equalized to determine the true range of that target.

## 8.2 Equalization Steps

Based on this discussion the equalization problem can be divided into two steps.

1. Separation of direct and multipath signals, of target of interest, from aggregate signal received.
2. Equalization of extracted signal to determine the true range of target.

Step 1, although not a simple problem in itself, can be done using advance signal processing techniques like blind signal separation (BSS) or adaptive beam forming of receiver antenna towards target of interest.

For step 2, linear equalizer (LE), which is an adaptive equalization technique when propagation channel is unknown, can be used to correct the target ranges. Digital waveforms commonly used in urban applications of passive radars contain known training sequence which is transmitted in packet header to combat the inter symbol interference (ISI). These training symbols are used as a reference for equalization process thus to mitigate the effects of multipaths. In 802.11b WiFi signals, 128 bits long preamble or 56 bits short preamble is transmitted in every packet as a known training sequence. It is reiterated that adaptive equalization process cannot be applied before carrying out step 1 if more than one target is present in environment, as is the case in setup 3, because equalizer will treat all targets as scatter objects which are giving rise to multipaths.

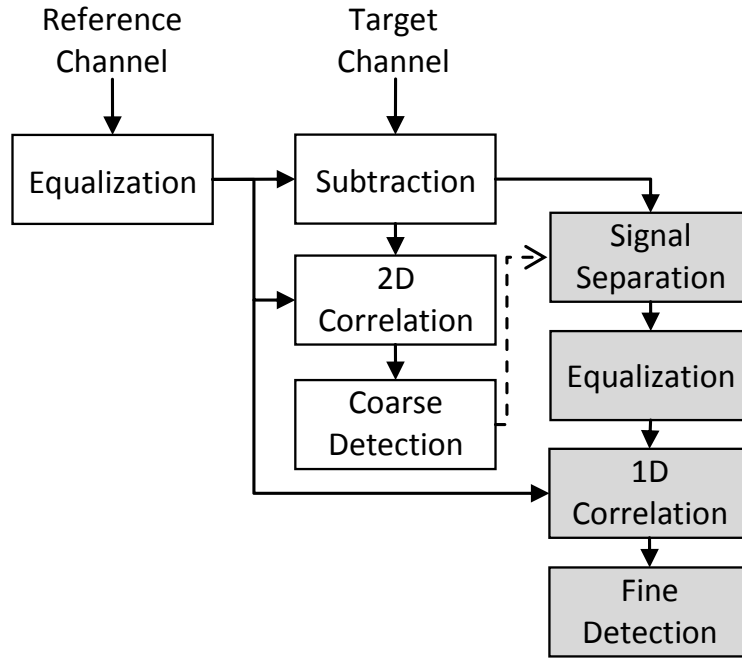


Figure 8.1: Process diagram for target detection in two phases

### 8.3 Proposed Algorithm

It is to be noted that the target detection process has now been divided in two phases. In the first phase, coarse target ranges and velocities of all available targets in the environment are calculated using 2D cross ambiguity function. This coarse target information is then utilized in the second phase to separate the targets of interest from composite received signal. The separated signal of each target of interest is processed through independent equalization processes to determine the true ranges using 1D cross ambiguity function matched to the Doppler frequency of target of interest.

The signal flow diagram for target detection in two phases is shown in Fig. 8.1. The reference signal is equalized to bring out the exact replica of transmitted signal and subtracted from target channel signal to remove DSI

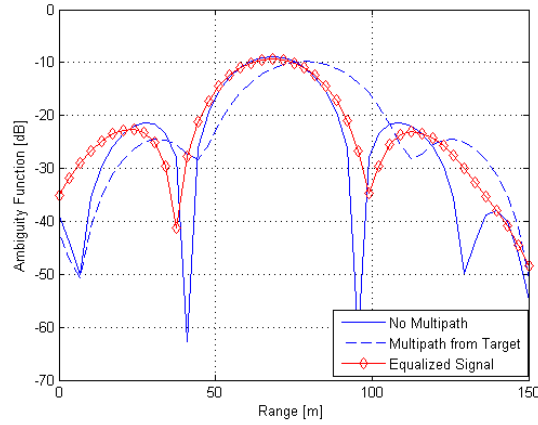


Figure 8.2: Offset target equalized for setup 1

and static clutter at 0 Hz Doppler frequency. A 2D cross ambiguity function (6.3) is calculated, followed by a detection algorithm to determine the coarse location and Doppler frequency of the targets available in the environment. Based on the coarse detection information, signal from targets of interest are separated and equalized to mitigate the effects of multipaths. 1D cross correlation function of equalized signal is calculated and true range of the target under evaluation is determined by fine detection algorithm.

To further comment, if targets of interest are separated through antenna beam forming, the targets can be localized using direction of arrival of signal, whereas, if step 1 is carried through BSS the corrected ranges may be passed to central processing station of multistatic passive radar system to determine the location of the targets of interest [11].

## 8.4 Application

Simulation setups 1 and 2 can be treated as simplified scenarios for equalization process in which step 1 of equalization problem has already been done,

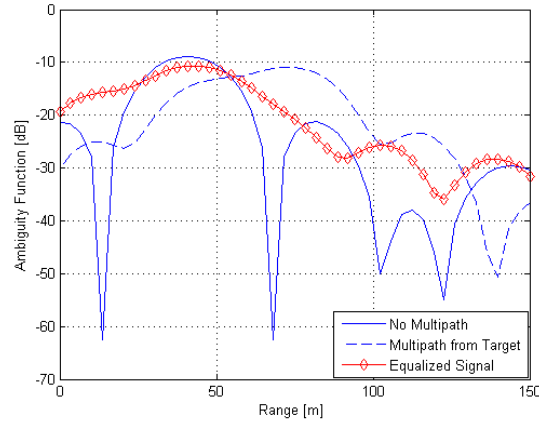


Figure 8.3: Smearing target equalized for setup 2

as  $s(t)$  contains only direct and multipath returns from a single target. An 8 tap symbol spaced adaptive linear equalizer [27], based on least mean square (LMS) algorithm with step size of 0.02, was applied to received signals of simulation setups 1 and 2, using long preamble as a training sequence.

The target range correction result for setup 1 is shown in Fig. 8.2. The target was actually present at  $68.1m$ , however when multipath signal from  $\Delta R = 20.45m$  was also received along with direct signal, the measured range was offset to  $78.4m$ . The linear equalizer corrected the targets to its true range, which is shown as red plot. Similarly, single target present at  $40.9m$  in setup 2 was smeared in range due to multipaths in ITU office model A channel, which was corrected by equalizer to its actual range as shown in red plot of Fig. 8.3.

# Chapter 9

## Conclusion

### 9.1 Conclusion

In urban sensing application of passive radars, multiple copies of target echoes can be received due to signal traveling through multipaths in rich scattering environment. Three different setups were studied to determine the effects of target multipaths. These target multipaths seriously degrade the range measurement accuracy, which results in target either offsetting from actual range, smearing in range dimension or ghost targets may appear, depending upon the range resolution of the selected waveform and relative path difference of multipath to direct signal path. It was observed that if relative path difference is less than twice the range resolution, all three range degradation may appear, whereas only ghost targets will appear if path difference is greater than double the range resolution.

It has been proposed that target detection is to be carried out in two phases, namely coarse detection and fine detection. For fine detection of targets in rich scattering environment, it has been demonstrated that a two step equalization process can accurately determine the true range of targets.

## 9.2 Major Contributions

- Development of Matlab code for ambiguity function, optimized for speed using parallel programming.
- Implementation of passive radars processing scheme.
- Simulation of GSM and WiFi signals.
- Development of target environment models.
- Application of equalizer on target returns which has not been done before by any researcher in this area.
- Development of algorithm to detect true target ranges in scattering rich environment.

## 9.3 Future Work

- Hardware implementation of WiFi-based passive radar using Software Defined Radios (SDR)
- Blind source separation of targets using higher order statistics
- Multipath equalization of separated targets based on proposed algorithm
- Target localization using multi-static passive radar configuration

# Bibliography

- [1] CJ Baker, HD Griffiths, and I Papoutsis. Passive coherent location radar systems. part 2: Waveform properties. *IEE Proceedings-Radar, Sonar and Navigation*, 152(3):160–168, 2005.
- [2] Christian R Berger, Bruno Demissie, Jörg Heckenbach, Peter Willett, and Shengli Zhou. Signal processing for passive radar using ofdm waveforms. *Selected Topics in Signal Processing, IEEE Journal of*, 4(1):226–238, 2010.
- [3] Roberta Cardinali, Fabiola Colone, Chiara Ferretti, and Pierfrancesco Lombardo. Comparison of clutter and multipath cancellation techniques for passive radar. In *Radar Conference, 2007 IEEE*, pages 469–474. IEEE, 2007.
- [4] Kevin Chetty, Graeme E Smith, and Karl Woodbridge. Through-the-wall sensing of personnel using passive bistatic wifi radar at standoff distances. *Geoscience and Remote Sensing, IEEE Transactions on*, 50(4):1218–1226, 2012.
- [5] Christopher John Coleman, RA Watson, and Heath James Yardley. A practical bistatic passive radar system for use with dab and drm illumin-

- nators. In *IEEE Radar Conference (2008: Rome, Italy) RADAR'08*, 2008.
- [6] Fabiola Colone, Paolo Falcone, Carlo Bongioanni, and Pierfrancesco Lombardo. Wifi-based passive bistatic radar: data processing schemes and experimental results. *Aerospace and Electronic Systems, IEEE Transactions on*, 48(2):1061–1079, 2012.
- [7] Fabiola Colone, Paolo Falcone, and Pierfrancesco Lombardo. Ambiguity function analysis of wimax transmissions for passive radar. In *Radar Conference, 2010 IEEE*, pages 689–694. IEEE, 2010.
- [8] Fabiola Colone, Diego Langellotti, and Pierfrancesco Lombardo. Dvb-t signal ambiguity function control for passive radars. *Aerospace and Electronic Systems, IEEE Transactions on*, 50(1):329–347, 2014.
- [9] Fabiola Colone, Debora Pastina, Paolo Falcone, and Pierfrancesco Lombardo. Wifi-based passive isar for high-resolution cross-range profiling of moving targets. *Geoscience and Remote Sensing, IEEE Transactions on*, 52(6):3486–3501, 2014.
- [10] Fabiola Colone, Karl Woodbridge, Hui Guo, David Mason, and Chris J Baker. Ambiguity function analysis of wireless lan transmissions for passive radar. *Aerospace and Electronic Systems, IEEE Transactions on*, 47(1):240–264, 2011.
- [11] Paolo Falcone, Fabiola Colone, Antonio Macera, and Pierfrancesco Lombardo. Two-dimensional location of moving targets within local areas using wifi-based multistatic passive radar. *IET Radar, Sonar and Navigation*, 8(2):123–131, 2014.

- [12] HD Griffiths. New directions in bistatic radar. In *Radar Conference, 2008. RADAR'08. IEEE*, pages 1–6. IEEE, 2008.
- [13] HD Griffiths and CJ Baker. Passive coherent location radar systems. part 1: performance prediction. *Radar, Sonar and Navigation, IEE Proceedings-*, 152(3):153–159, 2005.
- [14] J Homer, K Kubik, B Mojarrabi, ID Longstaff, E Donskoi, and M Cherniakov. Passive bistatic radar sensing with leos based transmitters. In *Geoscience and Remote Sensing Symposium, 2002. IGARSS'02. 2002 IEEE International*, volume 1, pages 438–440. IEEE, 2002.
- [15] IEEE 802.11 Working Group. Wireless lan medium access control (mac) and physical layer (phy) specifications, 1997.
- [16] Cyril-Daniel Iskander and Hi-Tek Multisystems. A matlab-based object-oriented approach to multipath fading channel simulation. *Hi-Tek Multisystems*, 21, 2008.
- [17] ITU-R Recommendation M.1225. Guidelines for evaluation of radio transmission technologies for imt-2000, 1997.
- [18] Joe J Johnson. Implementing the cross ambiguity function and generating geometry-specific signals. Master's thesis, Naval Postgraduate School Monterey CA, USA, 2001.
- [19] Krzysztof Kulpa, Mateusz Malanowski, and Piotr Samczynski. Multipath illumination effects in passive radars. In *Radar Symposium (IRS), 2011 Proceedings International*, pages 321–326. IEEE, 2011.

- [20] H Kuschel and D O'Hagan. Passive radar from history to future. In *Radar Symposium (IRS), 2010 11th International*, pages 1–4. IEEE, 2010.
- [21] J Palmer, S Palumbo, A Summers, D Merrett, S Searle, and S Howard. An overview of an illuminator of opportunity passive radar research project and its signal processing research directions. *Digital Signal Processing*, 21(5):593–599, 2011.
- [22] P Samczynski, K Kulpa, M Malanowski, P Krysik, and L Maslikowski. A concept of gsm-based passive radar for vehicle traffic monitoring. In *Microwaves, Radar and Remote Sensing Symposium (MRRS), 2011*, pages 271–274. IEEE, 2011.
- [23] SEECS, NUST. High performance computing lab, 2014. Accessed: 15 December, 2014 <http://hpc.seecs.edu.pk/hardware.php>.
- [24] Pawan Setlur, Giovanni Alli, and Luigia Nuzzo. Multipath exploitation in through-wall radar imaging via point spread functions. *Image Processing, IEEE Transactions on*, 22(12):4571–4586, 2013.
- [25] Pawan Setlur, Moeness Amin, and Fauzia Ahmad. Multipath model and exploitation in through-the-wall and urban radar sensing. *Geoscience and Remote Sensing, IEEE Transactions on*, 49(10):4021–4034, 2011.
- [26] Merrill I. Skolnik. *Radar Handbook*. McGraw-Hill, New York, 3 edition, 2008.
- [27] Gordon L. Stuber. *Principles of Mobile Communication*. Springer, New York, 3 edition, 2012.

- [28] Hongbo Sun, Danny KP Tan, and Yilong Lu. Aircraft target measurements using a gsm-based passive radar. In *Radar Conference, 2008. RADAR'08. IEEE*, pages 1–6. IEEE, 2008.
- [29] Hongbo Sun, Danny KP Tan, Yilong Lu, and Marc Lesturgie. Applications of passive surveillance radar system using cell phone base station illuminators. *Aerospace and Electronic Systems Magazine, IEEE*, 25(3):10–18, 2010.
- [30] DKP Tan, Hong-bo Sun, Yi-long Lu, M Lesturgie, and HL Chan. Passive radar using global system for mobile communication signal: theory, implementation and measurements. In *Radar, Sonar and Navigation, IEE Proceedings-*, volume 152, pages 116–123. IET, 2005.
- [31] Ching L Teo. Bistatic radar system analysis and software development. Master's thesis, Naval Postgraduate School Monterey CA, USA, 2003.

# Appendix A

## Matlab Code for Signal Generation

```
clear all; clc; close all;
Ts=3.692e-6;
Sample_Per_Symbol = 4;
Fs = Sample_Per_Symbol/Ts;

%%
%simulate GSM signal for 0.25 secs
TS_Power= [2 2 2 1 1 1 1 1];
TRAINING = [0 0 1 0 0 1 0 1 1 1 0 0 0 0 1 0 0 0 1 0 0 1
            0 1 1 1];
TAIL = [0 0 0];
CTRL = [1];
TS0 = round(rand(1,114));
hMod = comm.GMSKModulator( 'BitInput', true, '
    BandwidthTimeProduct', 0.3, 'PulseLength', 4, '
```

```

SymbolPrehistory', 1, ...
                                'InitialPhaseOffset', 0, '
                                SamplesPerSymbol',
                                Sample_Per_Symbol);

IQ = 0;
for m=1:55
    % fix data in TS0
    tx_burst = [TAIL TS0(1:57) CTRL TRAINING CTRL TS0
                (58:114) TAIL];
    burst = [xor(tx_burst(1:end-1),tx_burst(2:end))
            tx_burst(148)]; %differential encoding and copy
                           original bit at end
    reset(hMod);
    modop = step(hMod, burst');
    IQ = [IQ TS_Power(1)*modop' zeros(1,round(8.25*
        Sample_Per_Symbol))]; %last element is guard
                               period of 8.25 bit period

for n=2:8
    tx_data = round(rand(1,114));
    tx_burst = [TAIL tx_data(1:57) CTRL TRAINING
                CTRL tx_data(58:114) TAIL];
    burst = [xor(tx_burst(1:end-1),tx_burst(2:end))
            tx_burst(148)]; %differential encoding and
                           copy original bit at end
    reset(hMod);
    modop = step(hMod, burst');

```

```

        IQ = [IQ TS_Power(n)*modop' zeros(1,round(8.25*
            Sample_Per_Symbol))];    %last element is
            guard period of 8.25 bit period
    end

end

IQ = IQ(2:end);    % remove the first bit which was
    added at start of simulation
%%
% Introduce fading channel and add AWGN
chan = rayleighchan(Ts,0);
chan .DopplerSpectrum = doppler.gaussian(.3);
IQ = filter(chan ,IQ);
hAWGN = comm.AWGNChannel('NoiseMethod', 'Signal to
    noise ratio (SNR)', 'SNR',20);
IQ= step(hAWGN, IQ);

%%
% Plot the time domain view for 0.25 sec
L = length(IQ);
t = (0:L-1) /Fs ;
plot(t ,real(IQ));
axis([-0 .25 -3 3])
xlabel('Time [Sec] ');
ylabel('Level [Volt] ');
title('Received Downlink Signal');

```

```

grid on

%%
% Plot the time domain view of one frame
figure
plot(t, abs(IQ));
axis([-0 .0045 0 3])
xlabel('Time [Sec]');
ylabel('Absolute Level [Volt]');
title('Received GSM Frame');
grid on

%%
%Symbol Rate calculation
IQ_SQR = abs(abs(real(IQ)).^2).^2;
f1=250e3; %start freq for Chirp z-transform
f2=300e3; %stop freq for Chirp z-transform
m = length (IQ_SQR);
w = exp(-1i*2*pi*(f2-f1)/(m*Fs));
a = exp(1i*2*pi*f1/Fs);
IQ_frequency_domain = czt(IQ_SQR,m,w,a);
LFFT = length(IQ_frequency_domain);
IQ_frequency_domain = IQ_frequency_domain / LFFT; %
    Division by FFT length (based on MATLAB's FFT
    implementation)
freq_vector = ((0:LFFT-1)')*(f2-f1)/LFFT) + f1;
figure

```

```

plot( fftshift (freq_vector) , fftshift (IQ_frequency_domain
    ) );
[~, I] = max(IQ_frequency_domain(5:LFFT) );
sym_rate = (I * (f2-f1)/ LFFT + f1);
str = num2str(sym_rate/1000, '\nSymbol Rate (ksps) =
    %.3f\n');
title(str);
ylabel('Absolute Level');
xlabel('Symbol Rate[sps]');

%%
% Plot the spectrum of GSM signal
IQ_frequency_domain = fft(IQ);
LFFT = length(IQ_frequency_domain);
IQ_frequency_domain = IQ_frequency_domain / LFFT; %
    Division by FFT length (based on MATLAB's FFT
    implementation)
P_frequency_domain_W = (abs(IQ_frequency_domain)).^2 /
    50; %  $P = U^2 / R$ 
P_frequency_domain_dBm = 10*log10( P_frequency_domain_W
    / 1e-3 ); %  $P [dBm] = 10*log_{10}(P/1mW)$ 
freq_vector = (0:LFFT-1) / LFFT;
freq_vector(freq_vector >=0.5) = freq_vector(freq_vector
    >=0.5) - 1; % Frequency vector
freq_vector = (freq_vector * Fs); % Frequency vector in
    Hz
figure

```

```

plot(fftshift(freq_vector),fftshift(
    P_frequency_domain_dBm));
grid on;
xlabel('Frequency [Hz] (relative to the center
    frequency)');
ylabel('Level [dBm]');
title('GSM Downlink Signal');
%%
figure
[S,F,T,P] = spectrogram(IQ,256,100,512,Fs);
freq_vector = (0:512-1) / 512;
freq_vector(freq_vector >=0.5) = freq_vector(freq_vector
    >=0.5) - 1; % Frequency vector
freq_vector = (freq_vector * Fs); % Frequency vector in
    Hz
surf(T,fftshift(freq_vector),fftshift(10*log10(P)),',
    edgecolor','none'); axis tight;
title('Spectrogram GSM Simulated Signal')
xlabel('Time [sec] ');
ylabel('Frequency [Hz] ');
zlabel('Level [dB] ');
%
%%
%Ambiguity in Range Resolution
tau = -5e-3:5e-6:5e-3; %Time Delay
range = zeros(length(tau));
expanded_IQ = [zeros(1,ceil(Fs*max(abs(tau)))) IQ

```

```

    zeros(1, ceil(Fs*max(abs(tau))))];
L=length(IQ);
for n=1:length(tau)
    x = round(Fs*max(abs(tau))+1+Fs*tau(n));
    y = round(Fs*max(abs(tau))+Fs*tau(n))+L;
    shifted_IQ=expanded_IQ(x:y);
    range(n)= sum( IQ .* conj(shifted_IQ) ) /L;
    range(n) = 10*log10( abs(range(n))^2 );
end
plot(tau, range);
title('Ambiguity in Range Resolution (Time Delay)')
xlabel('Time Delay [sec] ');
ylabel('Level [dB] ');
grid on
%%
%Ambiguity in Velocity Resolution
phi = -500:1:500; %(Doppler Shift Hz)
doppler = zeros(length(phi));
for m=1:length(phi)
    vel_shift = exp(-1j* (2*pi*phi(m)/Fs) *(1:length(IQ)
    ));
    doppler(m)= sum( IQ .* conj(IQ) .* vel_shift ) /
    length(IQ);
    doppler (m) = 10*log10( abs(doppler(m))^2 );
end
figure
plot(phi, doppler);

```

```

title('Ambiguity in Velocity Resolution (Doppler Shift)
      ')
xlabel('Doppler Shift [Hz] ');
ylabel('Level [dB] ');
grid on

%%
%Ambiguity Function 3D op, Very slow processing
tau = -5e-3:5e-5:5e-3;
phi = -500:5:500;
op = zeros(length(tau), length(phi));
expanded_IQ = [zeros(1, ceil(Fs*max(abs(tau)))) IQ
              zeros(1, ceil(Fs*max(abs(tau))))];
L=length(IQ);
Max_Shift = Fs*max(abs(tau));
vel_shift=zeros(1,L);
for n=1:length(tau)
    x = round(Max_Shift +1+Fs*tau(n));
    y = round(Max_Shift+Fs*tau(n)) + L;
    shifted_IQ=expanded_IQ(x:y);
    for m=1:length(phi)
        vel_shift = exp(-1j* (2*pi*phi(m)/Fs) *(1:L));
        op(n,m)= sum( IQ .* conj(shifted_IQ) .*
                    vel_shift ) / L;
        op(n,m) = 10*log10( abs(op(n,m))^2 );
    end

```

```
end
```

```
%%
```

```
h1=figure;
```

```
h=surf(3e8*tau, phi, op);
```

```
set(h, 'LineStyle', 'none');
```

```
grid on
```

```
title('Ambiguity Function GSM Signal')
```

```
ylabel('Doppler Shift [Hz]');
```

```
xlabel('Range [m]');
```

```
zlabel('Level [dB]');
```

# Appendix B

## 3D Ambiguity Function

```
function [phi , tau , op]=caf3D (IQ1 ,IQ2 ,Fs ,MaxRange ,
    MaxDoppler)
c=3e8 ;
MaxTau= MaxRange/c ;
tau = 0 : 1/Fs: MaxTau;
phi = -MaxDoppler : 2*MaxDoppler/(length(tau)-1):
    MaxDoppler ;
L=length(IQ1) ;
Lp=length(phi) ;
Lt=length(tau) ;
op = zeros(Lp,Lt) ;
parfor m=1:Lp
    expanded_IQ2 = IQ2;
    vel_shift = exp(-1j* (2*pi) *((1:L)) * phi(m)/Fs);
    temp1 = IQ1.*vel_shift ;
    Opt= zeros(1, Lt);
    for n=1:Lt
```

```
    Opt(n) = sum( temp1 .* conj(expanded_IQ2));  
    expanded_IQ2 = [0 expanded_IQ2(1:end-1)];  
end  
    op(m,:) = Opt;  
end  
op = op/norm(op);  
op=10*log10(abs(op).^2);
```

# Appendix C

## 1D Ambiguity Function

```
function [tau , op]=caf1D(IQ1,IQ2,Fs,MaxRange,phi)
c=3e8;
MaxTau= MaxRange/c;
tau = 0 : 1/Fs: MaxTau;
L= length(IQ1);
op = zeros(1,length(tau));
length(tau);

vel_shift = exp(-1j* (2*pi) *(1:L) * phi/Fs);
IQ= IQ1.*vel_shift ;

for n=1:length(tau)
    op(n)= sum( IQ.* conj(IQ2));
    IQ2 = [0 IQ2(1:end-1)];
end

op = op/norm(op);
```

```
op=10*log10(abs(op).^2);
```

# Appendix D

## Passive radar processing

```
clear all;
clc;
clear global
close all

load IQ_beacon_Long;
IQ = IQ(1:2^(nextpow2(length(IQ))-5));
% IQ=IQ(45127:79310);
up=1;
IQ = interp(IQ,up);
Fs=Fs*up;
visual(IQ,Fs);
axis[0 .01 -1 1]
tgt = IQ;
ref = IQ;
clear IQ;
%%
```

```

c=3e8;
fc = 2437e6;
lamda = c / fc;
L=length(tgt);

h0 = zeros(1,30);
range= 44;
doppler=50;
delay = floor(range*Fs/c)/Fs;
range = delay*c;
RangeTarget = range;
phase = exp(1j* ( 2*pi*doppler/Fs - 2*pi*3e8*delay/
    lamda));
h0(round(delay*Fs+1))=phase;

Ts = 1/Fs;
DeltaR = Ts*c;
disp(['Fs=' num2str(Fs) ' Ts=' num2str(Ts) ' DeltaR='
    num2str(DeltaR)]);
disp(['Tsym=' num2str(1/11e6) ' Rres=' num2str(c/(2*11
    e6))] );
disp(' ');
disp(['Range h0 =' num2str(range) ' Doppler =' num2str(
    doppler) ' Delay=' num2str(delay)]);
% disp(' ');
%%

```

```

h1 = zeros(1,30);
i=3;
range= 80;
doppler=70;
delay = floor(range*Fs/c)/Fs;
range = delay*c;
phase = exp(1j* ( 2*pi*doppler/Fs - 2*pi*3e8*delay/
    lamda));
h1(round(delay*Fs+1))=phase;
disp([ 'Range h1=' num2str(range) ' Doppler =' num2str(
    doppler) ' Delay=' num2str(delay)]);
disp(' ');
%

i=6;
h2 = zeros(1,30);
range= RangeTarget+i*DeltaR;
delay = floor(range*Fs/c)/Fs;
phase = exp(1j* ( 2*pi*doppler/Fs - 2*pi*3e8*delay/
    lamda));
h2(round(delay*Fs+1))=0.5*phase;
disp([ 'Range h2=' num2str(range) ' Doppler =' num2str(
    doppler) ' Delay=' num2str(delay)]);

h=h0+h1+h2;
impz(abs(h));

```

```

Hd = dfilt.dffir(h);
zplane(Hd)

tgt0=conv(tgt,h0);
tgt0=tgt0(1:L);

tgtm=conv(tgt,h0);
tgtm=(tgtm(1:L));

chan = stdchan(1/Fs, 0, 'itur3GIAx');
% chan.NormalizePathGains = 1;
% chan.StoreHistory=1;
tgtm=filter(chan, tgtm);

eqlms = lineareq(8,lms(0.02));
eqlms.nSampPerSym=8;
tgte = equalize(eqlms,tgtm,ref(1:1536));
tgte = interp(tgte,8);

MaxRange = 150;
Doppler= 70;
[tau, op0]=caf1D(tgt0,ref,Fs,MaxRange,Doppler);
[tau, opm]=caf1D(tgtm,ref,Fs,MaxRange,Doppler);
[tau, ope]=caf1D(tgte,ref,Fs,MaxRange,Doppler);

```

```

[val index]=max(opm);
disp(['Equalizer Output Max = ' num2str(tau(index)*3e8)
    ]);
disp(' ');
% figure
hold off
h=plot(tau*3e8, op0, '-');
hold on
plot(tau*3e8, opm, '—');
plot(tau*3e8, ope, '-dr');
grid on
xlabel('Range [m] ');
ylabel('Ambiguity Function [dB]');
legend('No Multipath', 'Multipath from Target', '
    Equalized Signal');

%%
MaxRange = 1000;
MaxDoppler= 1000;
matlabpool close force local
matlabpool('open',2);
% ticki
[phi,tau, op]=caf3D(tgtm, ref, Fs, MaxRange, MaxDoppler);
% toc
matlabpool('close');

```

```
%  
close all;  
h1=figure;  
surf(3e8*tau , phi , op)  
grid on  
title( 'Ambiguity Function ' )  
ylabel( 'Doppler Shift [Hz] ' );  
xlabel( 'Range [m] ' );  
zlabel( 'Level [dB] ' );  
axis( [0 MaxRange -MaxDoppler MaxDoppler] )  
view( [0 90] );
```